DESIGN OF A RECEPTANCE-BASED ACTIVE AEROELASTIC CONTROLLER IN THE PRESENCE OF PARAMETRIC UNCERTAINTIES

S. Fichera[*] , T.A.M. Guimarães[**] , S. Jiffri[***] , D.A. Rade[****] , J.E. Mottershead[*]
[*]University of Liverpool, School of Engineering, Liverpool L69 3GH, United Kingdom , [**]UFU - Federal University of Uberlândia, School of Mechanical Engineering, Brazil , [***]Swansea University, College of Engineering, Swansea SA2 8PP, United Kingdom , [****]ITA - Technological Institute of Aeronautics, Division of Mechanical Engineering, Brazil

Keywords: *Active Aeroelastic Control, Receptance Method, Uncertainty propagation, Polynomial Chaos Expansion*

Abstract

This paper presents a numerical investigation of the effects of parametric uncertainties propagated through Polynomial Chaos Expansion on the design of a Receptance-based active controller for aeroelastic systems. The test-case is representative of an experimental rig featuring a subsonic flexible wing with multiple control surfaces. The uncertainty is introduced in the Young's modulus of the main spar. Such uncertainty is firstly propagated to assess the open loop behavior of the aeroelastic system in terms of flutter velocity and frequency responses. A Receptance-based controller is then designed deterministically with the goal of increasing the flutter boundary and its performance is tested against the uncertain aeroelastic system. Finally, the PDFs of the receptance control gains are evaluated and discussed.

1 Introduction

The presence of uncertainties in aeroelastic systems has been carefully reviewed by Beran et al. in [1], the authors highlight the importance of addressing it both from a structural and an aerodynamic prospective, the latter being not subject of this works. The ability of modeling it as part of the aeroelastic design is essential when flutter mechanisms are closely spaced [7] or when in presence of nonlinearities [4]. Manan et al. [3] looked to the problem of uncertainty in the structural parameters of and aeroelastic model via stochastic expansion methods in the frequency domain.

This work, in the context of aeroelasticity, parametric uncertainties and active control, attempts to evaluate the Receptance Method [5] in the presence of aleatory uncertainty for the design of an Active Aeroelastic Controller (AAC), to understand its limits and to propose a way forward. The propagation technique used for this study is Polynomial Chaos Expansion (PCE) [8]. A numerical model, based on an underlying Finite Element model coupled with unsteady aerodynamic, describing the MODular FLEXible aeroelastic wing (MODFLEX) apparatus [2], is adopted in the present investigation.

The paper is divided as follows: after the above introduction, Section 2 presents the numerical MODFLEX model used for investigating the problem, Section 3 discusses the Polynomial Chaos (PC) expansion used for addressing the propagation of the uncertainties, while Section 4 introduces the Repentance Method (RM) used for partially assigning the poles of the system. The results are discussed in Section 5, followed by the conclusions in Section 6.

2 Description of the numerical aeroelastic model

As anticipated in the introduction, the proposed procedure is implemented on the twin numerical model of the MODFLEX experimental rig. The MODFLEX apparatus has been developed in the recent years at the University of Liverpool as a test-bench for experimental investigations of active control strategies in aeroelastic systems. The rig is representative of a flexible wing with multiple control surfaces; the main structure is composed by a load-bearing aluminum alloy spar to which are single-point connected four aerodynamic sectors and a tip sector, as shown in Figure 1. The main specifications of the MODFLEX aeroelastic flexible wing are summarized in Table 1.

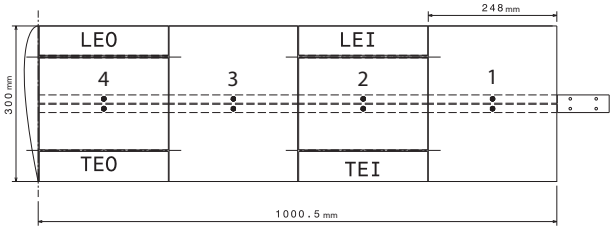

Fig. 1 : MODFLEX drawing.

Table 1: MODFLEX main specifications.

wing data	dimension
wing span	1 m
wing sector	0.248 m
sector chord (c)	0.3 m
aerofoil	NACA 0018
mass axis position	0.5 x c
flexural axis position	0.5 x c

The experimental model has a numerical twin which features a Finite Element beam structure coupled with potential aerodynamics (Doublet Lattice - DLM). Numerical analyses and wind tunnel tests showed that the aeroelastic wing experiences a typical bending-torsional flutter instability at a wind speed of $V_f = 13$ m/s. A detailed description of the rig can be found in [2]. In this work, all the structural and aerodynamic information for both assessing the uncertainty propagation and for designing the Receptance-based controller are computed with Nastran/DMAP [6]. The configuration used in this work features a single input, the Trailing Edge Outer (TEO), and two displacement outputs, perpendicular to the plane of the wing, located at three quarters of the span of the wing, ahead (OP1) and aft (OP2) the main spar. This has been done for assuring consistency with previous experimental works of the same authors, see [2]. However, the procedure can be immediately extended for the MIMO case. Using a generic formulation, the aeroelastic system can be described as follows

$$\boldsymbol{M_s}\ddot{\boldsymbol{q}} + \boldsymbol{C_s}\dot{\boldsymbol{q}} + \boldsymbol{K_s}\boldsymbol{q} = q\boldsymbol{f_a} + \boldsymbol{f_m} \tag{1}$$

where $\boldsymbol{M_s}$, $\boldsymbol{C_s}$, and $\boldsymbol{K_s}$ are the mass, damping, and stiffness structural matrices, respectively; $\boldsymbol{f_a}$ is the vector of generalized aerodynamic forces (GAFs), $\boldsymbol{f_m}$ represents the external force, q is the dynamic pressure and $\boldsymbol{q}$ is the vector of the system states. The dimension of the generalized model that indicates the number of modes retained is m; specifically, the first mode represents the static deflection of the trailing edge outer and the remaining nine the elastic modes of the system. The GAFs are computed in the reduced-frequency k domain by using the classical DLM theory, which is

$$\boldsymbol{f_a} = \boldsymbol{H}_{am}(k; M_\infty)\boldsymbol{q}. \tag{2}$$

Since the $\boldsymbol{H}_{am}(k; M_\infty)$ is computed in a discrete manner, an interpolation is necessary for evaluating the unsteady aerodynamics on the entire domain of interest. Eq. 1 can be rewritten as follows by moving to the LHS the aerodynamic term

$$\begin{aligned}\boldsymbol{M_s}\ddot{\boldsymbol{q}} + (\boldsymbol{C_s} - q(\frac{c}{2V}) \cdot real(\boldsymbol{H}_{am}))\dot{\boldsymbol{q}} + \\ (\boldsymbol{K_s} - q \cdot img(\boldsymbol{H}_{am}))\boldsymbol{q} = 0.\end{aligned} \tag{3}$$

By taking the inverse of the LHS of Eq. 3, and pre- and post-multiplying by the eigenvectors matrix after having opportunely selected the single-input and multiple-output nodes, the transfer functions in physical coordinates can be evaluated. Figure 2 shows the FRF evolution ob-

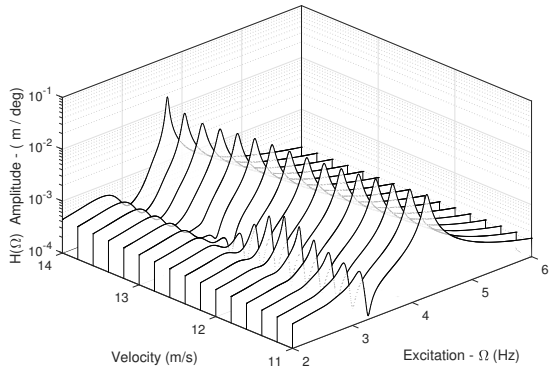

Fig. 2 : MODFLEX FRF evolution with velocity for deterministic case - OP1.

tained for the first output point, between an airflow speed of 11m/s up to 14m/s, for the deterministic solution. It is evident that that the modes coalesce approximately at 12.5m/s.

3 Propagation of uncertainty though the model

The MODFLEX numerical model is augmented by introducing an uncertainty in the value of the main-spar elastic modulus. The influence of parameter uncertainty on the aeroelastic stability is then investigated using the classical Polynomial Chaos Expansion (PCE) technique [8] which main polynomial is reported in Eq. 4 that expresses the response for one parameter in one dimension

$$u = \beta_0 + \beta_1\xi + \beta_2(\xi^2 - 1) + \beta_3(\xi^3 - 3\xi) + \beta_4(\xi^4 - 6\xi^2 + 3) + \ldots \quad (4)$$

where ξ is the independent standard Gaussian random variable, in this case the Young's modulus, and β_i are the terms of the orthogonal polynomial. Specifically, Hermite polynomials have been used and the elastic modulus (assumed to be Gaussian) is defined by a standard deviation, σ, equal to 3.3% of the nominal value. The Latin-hypercube sampling technique is used for selecting a small sample of individuals ($N = 20$), for which the solution of the aeroelastic problem was computed numerically. The PC expansions were then fitted by using the same base but changing the surrogate outputs in relation to the different stage of the investigation. Initially a surrogate model was created for evaluating the envelope of the V-g flutter diagram (as shown hereinafter in Subsection 3.1). Subsequently, the same sample of individuals was used to create the PDFs of the Receptance-based controller gains.

3.1 V-g flutter diagram for the expanded model

Due to the aeroelastic behavior shown by MODFLEX, the first two modes are considered the most relevant for this study, whereas the third is retained for verification purposes. This led to 3 x 2 polynomials (frequency and damping) expansion of the 2^{nd} order to be computed. The V-g

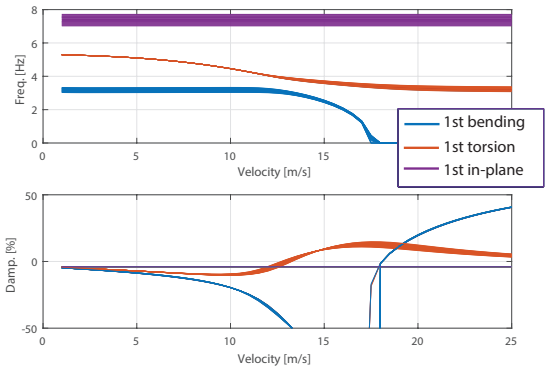

Fig. 3 : V-g flutter diagram due to a parametric uncertainty in the Young's modulus.

flutter diagram bounds shown in Figure 3 were then computed by evaluating such polynomials for a 1000 sampling points. It is evident that the uncertainty on the elastic modulus has the effect of propagating an uncertainty on the flutter velocity (bounds 12.7 - 13.3 m/s), being the PFD solution highlighted in Fig. 4; it is interesting to notice here that the probability of flutter onset is slightly higher for lower velocities. Moreover, from a closer inspection of the diagram, it is evident that the most significant effect is on the natural frequency of the first bending mode that results in a spread of the zero-crossing position of the damping of the torsional mode.

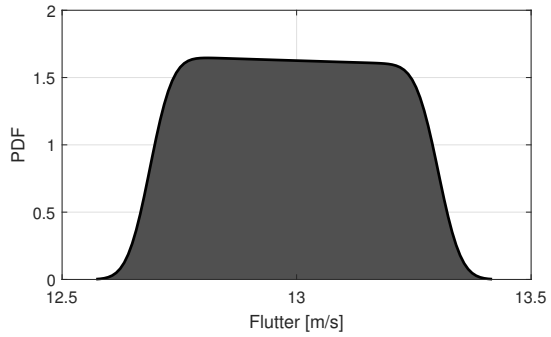

Fig. 4 : PDF for flutter onset.

3.2 Uncertain Frequency Response Function (UFRF)

Following a similar procedure to that described above, and in a similar manner to the approach presented by Manan et al. [3], where PCE was used to fit the coefficients of the polynomial function representing the system response, the envelope of the uncertain frequency response functions at incremental airflow velocities have been computed, as shown Fig. 5. A close inspection enables one to conclude that the first vibration mode, which represents the first bending mode, is more susceptible to the uncertainty in the elastic modulus. Moreover, as the airflow velocity increases, it becomes evident that coalescence occurs as the second mode migrates towards the first. In fact, the aeroelastic uncertainty propagation leads to a stochastic transfer function, and mainly the poles and zeros for the first mode (bending mode), as expected, are more susceptible. Figures 5.a, 5.b and 5.d depict the FRFs a two velocities below the flutter speed and one above, in all the cases the first peak is the most affected by the uncertainty, however, the overall shape of the FRFs is not significantly impacted by the variation of the elastic modulus. Of specific interest is instead Fig. 5.c that shows the FRF envelope in proximity of the flutter velocity. At this airspeed, even a small change in the elastic modulus can trigger the transition from a stable to an unstable condition, with the disappearance of the first peak.

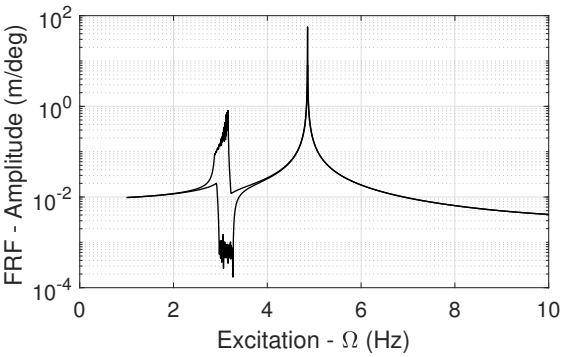

(a) Airspeed = 5 (m/s)

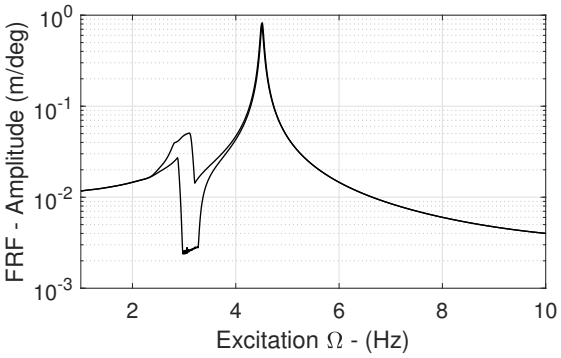

(b) Airspeed = 10 (m/s)

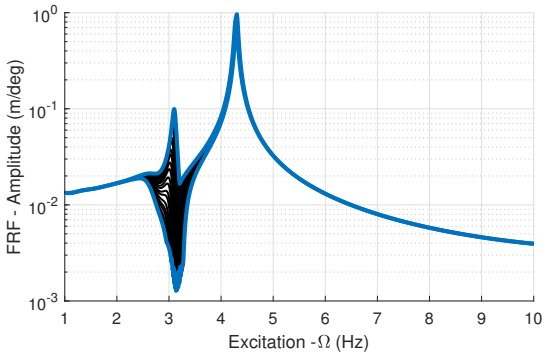

(c) Airspeed = 12 (m/s)

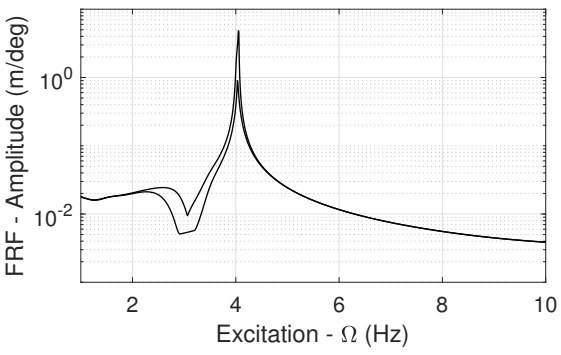

(d) Airspeed = 14 (m/s)

Fig. 5 : Stochastic FRF results for different values of airspeed - OP1.

4 Uncertainty propagation to the Receptance-based controller

The final step of this procedure sees the implementation of a feedback controller aimed at increasing the flutter velocity of the aeroelastic system. This reflects numerically what was experimentally validated recently by the same authors in [2]. The main contribution of this work is that the uncertainty is included in the model and its effects are propagated to the controller design. The controller design method chosen for computing the feedback gains is the so-called Receptance Method developed by Ram and Mottershead [5] and its main strength lies in not requiring any direct knowledge of the system besides the frequency response function at the locations of the poles. The receptance method is applicable to any frequency response function, but is readily understood in terms of receptances. Consider a generic dynamic system which receptance matrix is $\mathrm{H}(s)$ that has open loop eigenpairs equal to $\{\lambda_k, \quad \mathbf{v}_k\}$ for $k = 1,2,\ldots,2n$. Via partial-state feedback, proportional to displacements (g_m) and velocities (f_m), p eigenvalues μ_k for $k = 1,2,\ldots,p$ can be assigned while the remaining, $\mu_k = \lambda_k$ for $k = p+1, p+2, \ldots, 2n$, are retained. It has been demonstrated in [5] that, by defining

$$\mathbf{r}_{\mu_k,j} = \mathbf{H}(\mu_k)\mathbf{b}_j \quad j = 1,2,\ldots,m \tag{5}$$

with $\mathbf{b}_j$ input distribution vector and m number of inputs, and

$$\alpha_{\mu_k,j} = (\mu_k \mathbf{f}_j{}^T + \mathbf{g}_j{}^T)\mathbf{w}_k \quad \begin{matrix} k = 1,2,\ldots,p \\ j = 1,2,\ldots,m \end{matrix} \tag{6}$$

the part of the system related to the assigned poles can be expressed as

$$\mathbf{w}_k = \alpha_{\mu_k,1}\mathbf{r}_{\mu_k,1} + \alpha_{\mu_k,2}\mathbf{r}_{\mu_k,2} + \cdots + \alpha_{\mu_k,m}\mathbf{r}_{\mu_k,m} \qquad k = 1,2,\ldots,p. \tag{7}$$

The problem can be rewritten in matrix form in Eq. 8, where $\mathbf{P}_k$ and $\mathbf{Q}_k$ matrix are defined in 9, and the values of the gains are computed after a judicious choice of $\alpha_{\mu_k,j}$.

$$\begin{bmatrix} \mathbf{P}_1 \\ \vdots \\ \mathbf{P}_p \\ \mathbf{Q}_{p+1} \\ \vdots \\ \mathbf{Q}_{2n} \end{bmatrix} \begin{pmatrix} \mathbf{f}_1 \\ \vdots \\ \mathbf{f}_m \\ \mathbf{g}_1 \\ \vdots \\ \mathbf{g}_m \end{pmatrix} = \begin{pmatrix} \alpha_1 \\ \vdots \\ \alpha_p \\ \mathbf{0} \\ \vdots \\ \mathbf{0} \end{pmatrix} \tag{8}$$

$$\begin{cases} \mathbf{P}_k = \begin{bmatrix} \mu_k\mathbf{w}_k^T & 0 & \ldots & 0 & \mathbf{w}_k^T & 0 & \ldots & 0 \\ 0 & \mu_k\mathbf{w}_k^T & \ldots & 0 & 0 & \mathbf{w}_k^T & \ldots & 0 \\ \vdots & \vdots & \ddots & \vdots & \vdots & \vdots & \ddots & \vdots \\ 0 & 0 & \ldots & \mu_k\mathbf{w}_k^T & 0 & 0 & \ldots & \mathbf{w}_k^T \end{bmatrix} \\ \mathbf{Q}_k = \begin{bmatrix} \lambda_k\mathbf{v}_k^T & 0 & \ldots & 0 & \mathbf{v}_k^T & 0 & \ldots & 0 \\ 0 & \lambda_k\mathbf{v}_k^T & \ldots & 0 & 0 & \mathbf{v}_k^T & \ldots & 0 \\ \vdots & \vdots & \ddots & \vdots & \vdots & \vdots & \ddots & \vdots \\ 0 & 0 & \ldots & \lambda_k\mathbf{v}_k^T & 0 & 0 & \ldots & \mathbf{v}_k^T \end{bmatrix} \end{cases} \tag{9}$$

4.1 PCE of the controller gains

The Receptance Method briefly presented above has been implemented in the numerical procedure developed within this work for assigning frequency and damping of the poles associated with the first bending and first torsion mode, with the aim of increasing the flutter velocity of the system. As described in Section 2, the aeroelastic system features a single input ($\mathbf{b}_j = \mathbf{b}_1$) and two outputs. The receptance matrix is computed together with input distribution vector $\mathbf{b}_1$ and constitutes the $\mathbf{r}_{\mu_k,1}$ matrix presented in Eq. 5. Such matrix represents the two FRFs between the two outputs and the single input. The FRFs are computed at an airspeed of 10m/s that assures a safety margin with respect to the deterministic flutter velocity. The target of the aeroelastic controller is to increase the damping of both poles by 10% and to reduce the frequency of the first (bending) by 10% while increasing that of the second mode (torsion) by the same amount, always with respect to the deterministic case. The stochastic results and the procedure are highlighted in Fig. 6. Even if the controller has always the same objective, the FRFs change due to the uncertainty in the elastic modulus and consequently the gains also change. A PCE, based on the same sample of individuals discussed in Section 3, was used for

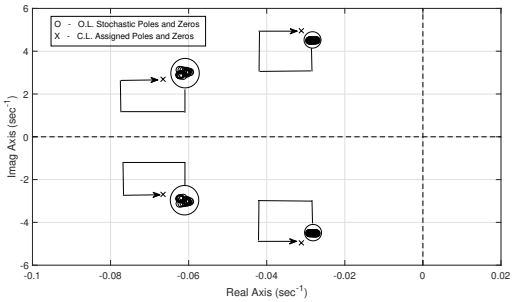

Fig. 6 : MODFLEX pole-zero map from stochastic results for the first two pairs of poles.

deriving the surrogate model of the Receptance-based controller design procedure. Once such a model is constructed, it is possible to evaluate the $\mathbf{f}_m$ and $\mathbf{g}_m$ gains on the entire domain of interest and compute their PDFs, as shown in Fig. 7.

5 Discussion of the Results

The analyses presented highlight the potential detrimental impact of uncertainty in the elastic modulus on the onset of flutter instability. Figure 3 shows the range of airspeed in which the flutter can occur, while Fig. 5.c, by representing the envelope of FRFs near the flutter velocity, highlights the transition between a stable and an unstable behavior. Figure 7 shows the PDF for the two pairs of gains due to the considered uncertainty. As expected, and in agreement with the previous experimental activities, the $\mathbf{f}_1$ and $\mathbf{f}_2$ gains, that are in feedback to the velocity, are smaller compared to $\mathbf{g}_1$ and $\mathbf{g}_2$ gains that are in feedback to the displacements. This ratio, of course, depends by the choice of the placed poles, and it can be different if the controller objective is not to increase the flutter stability margin of the system. Figure 8 shows the auto- and cross-correlation of the gains distributions and highlights the linear relationship between the $\mathbf{f}$ gains as well as between the $\mathbf{g}$ gains, while is evident that the cross-relationships are non-linear. One possible use of this information is to choose, for the uncertain system, the pairs of gains that have the highest PDFs (by using in conjunction with Figs. 7 and 8) and this will lead to a system that, even if sub-optimal for the deterministic case, will be less sensitive to the uncertainty.

6 Conclusions

The results presented above are the first step towards a stochastic, Receptance-based, active aeroelastic controller. The variation in the flutter velocity due to the elastic modulus uncertainly, highlights the importance of considering it in the design of a controller. The procedure implemented in this work proved to be effective in propagating such uncertainty to the frequency response functions first, and to the controller gains later. PCE has been used at different levels for creating surrogate models that, in end, resulted in PDFs useful for gaining information on the controller gains. The proposed use of the auto- and cross-correlation matrix of the gains (Fig. 8) as mean for making the system less sensitive to the uncertainty, will be subject of further investigations.

References

[1] Philip Beran, Bret Stanford, and Christopher Schrock. Uncertainty Quantification in Aeroelasticity. *Annual Review of Fluid Mechanics*, 49(1):361–386, 1 2017.

[2] S Fichera, S Jiffri, and J E Mottershead. Design and wind tunnel test of a MODular aeroelastic FLEXible wing (MODFLEX). In *Proceedings of the International Conference on Noise and Vibration Engineering ISMA 2016*, Leuven, Belgium, 2016.

[3] A. Manan and J. E. Cooper. Prediction of uncertain frequency response function bounds using polynomial chaos expansion. *Journal of Sound and Vibration*, 329(16):3348–3358, 2010.

[4] Chris L. Pettit and Philip S. Beran. Effects of Parametric Uncertainty on Airfoil Limit Cycle Oscillation. *Journal of Aircraft*, 40(5):1004–1006, 9 2003.

[5] Y.M. M. Ram and J. E. Mottershead. Multiple-input active vibration control by partial pole placement using the method of receptances. *Mechanical Systems and Signal Processing*, 40(2):1–9, 2013.

[6] W.P. Rodden and E.H. Johnson. *MSC/NASTRAN*

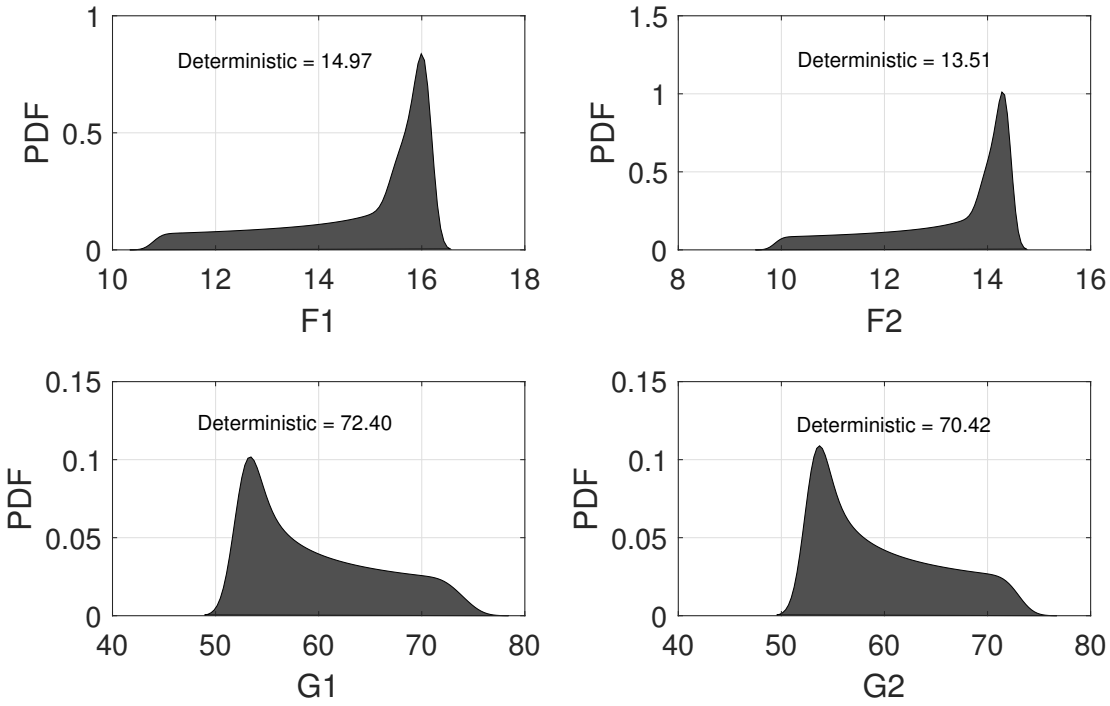

Fig. 7 : Stochastic gains PDF.

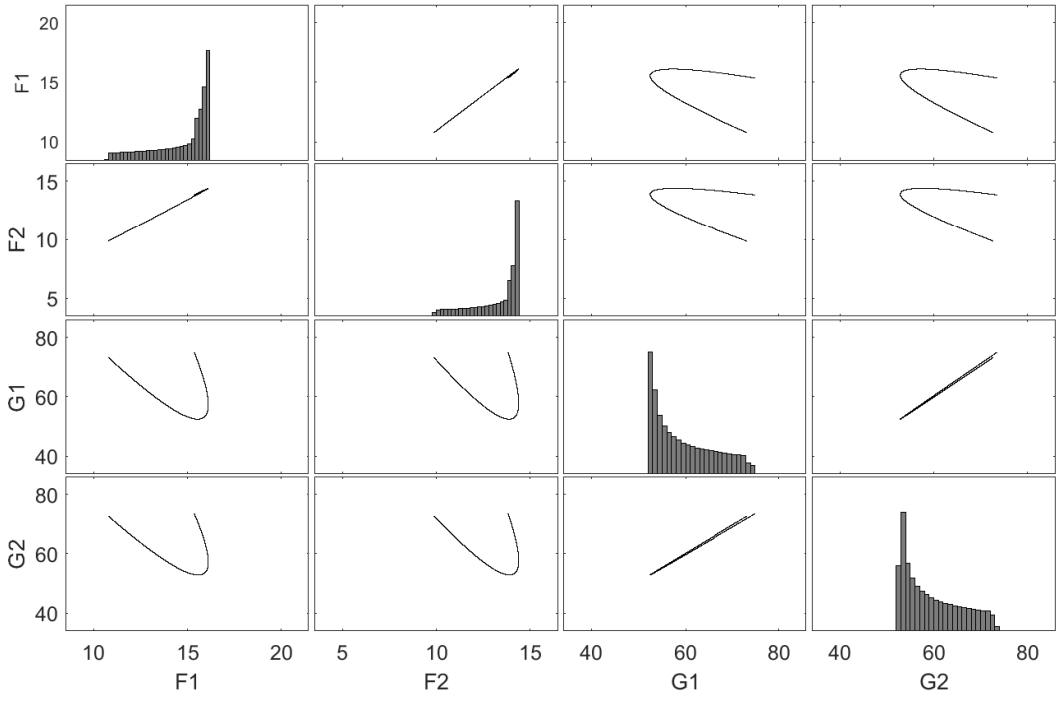

Fig. 8 : Stochastic gains auto- and cross-correlation.

Aeroelastic Analysis: User's Guide, Version 68. MacNeal-Schwendler Corporation, 1994.

[7] Carl Scarth, Jonathan E. Cooper, Paul M. Weaver, and Gustavo H C Silva. Uncertainty quantification of aeroelastic stability of composite plate wings using lamination parameters. *Composite Structures*, 116(1):84–93, 2014.

[8] N. Wiener. The Homogenous Chaos. *American Journal of Mathematics*, 60(4):897–936, 1938.

Contact Author Email Address

s.fichera@liverpool.ac.uk

Copyright Statement